



## Pediatric Radiology

## Dual energy head CT to maintain image quality while reducing dose in pediatric patients

Jason P. Weinman<sup>a,\*</sup>, David M. Mirsky<sup>a</sup>, Alexandria M. Jensen<sup>b</sup>, Nicholas V. Stence<sup>a</sup><sup>a</sup> Department of Radiology, Children's Hospital Colorado, 13123 E. 16th Ave., Box 125, Aurora, CO 80045, USA<sup>b</sup> Department of Biostatistics and Informatics, Colorado School of Public Health University of Colorado, Denver - Anschutz Medical Campus, 13001 E. 17th Place, Mail Stop B119, Aurora, CO 80045, USA

## ARTICLE INFO

## Keywords:

Head  
Brain  
CT  
Dual energy  
Dose reduction

## ABSTRACT

**Aim:** The aim of this study was to use dual energy CT technology to maintain or improve image quality in pediatric head CT while simultaneously reducing radiation dose.

**Materials and methods:** In this retrospective study, helical head CTs performed using a standard head CT protocol were compared to studies performed with a dual energy (DE) protocol. Objective comparison was performed by measuring regions of interest in 11 areas of the brain. Subjective rating for image quality using a Likert scale, was performed by three radiologists. Radiation doses were evaluated using CT dose index and dose length product.

**Results:** Signal-to-noise ratio was, for the most part, not significantly different between the DE and conventional scans. Contrast-to-noise ratio was slightly lower for children over 6 year of age utilizing the dual energy protocol versus the standard protocol.

Qualitatively, there was little difference in image quality in patients < 6 years old, with the only significant difference in infratentorial noise. However, in patients > 6 years of age, infratentorial noise, sharpness and diagnostic acceptability, as well as supratentorial sharpness were all significantly improved by DE CT technique. Radiation exposure as measured by CTDI and DLP was modestly lower with the dual energy protocol in all study populations.

**Conclusion:** Dual energy CT can be used clinically in pediatric patients to maintain or improve image quality while reducing radiation dose.

## 1. Introduction

The interaction of X-rays with matter is the core principle from which all radiographic imaging is based. It is the differential absorption and attenuation of X-ray beams that provides the contrast we use in radiographs and computed tomography (CT) to differentiate between various materials, such as gray and white matter, hemorrhage and brain, etc. At the energies typically used in radiographic and CT imaging, the photoelectric effect and Compton scatter are the predominant forces responsible for X-ray attenuation. The lack of scatter with the photoelectric effect makes it the most useful interaction in diagnostic imaging [1,2].

Photoelectric absorption is highly dependent upon the atomic number of the material. In material with high atomic number such as iodine ( $Z = 53$ ), and to a lesser extent calcium ( $Z = 20$ ), the photoelectric effect is the predominant interaction. In comparison to bone/

calcium ( $Z = 20$ ), soft tissue carbon ( $Z = 6$ ), hydrogen ( $Z = 1$ ) and oxygen ( $Z = 8$ ) have lower K-edge.

These differences in K-edges cause serious difficulties in head imaging due to the highly attenuating skull surrounding the lower attenuating brain. This leads to a problematic imaging trade-off: one can either image at a high kV to decrease image noise and artifact with resultant decreased image contrast, or image at a lower kV with improved image contrast but increased image noise and artifact.

Traditionally, this has been approached by imaging at an intermediate to high kV (often 120 kV) to maintain an acceptable level of image noise and contrast. Imaging at a low kV has been attempted to reduce dose in patients being evaluated for shunt dysfunction, although this results in increased image noise, especially within the posterior fossa [3]. More recently, imaging at a low kV with high milliamp seconds (mAs) has been evaluated to improve contrast while reducing dose. While partially successful, this results in increased noise -

\* Corresponding author.

E-mail address: [jason.weinman@childrenscolorado.org](mailto:jason.weinman@childrenscolorado.org) (J.P. Weinman).<https://doi.org/10.1016/j.clinimag.2019.02.005>

Received 10 August 2018; Received in revised form 5 February 2019; Accepted 6 February 2019

0899-7071/© 2019 Elsevier Inc. All rights reserved.

especially within the posterior fossa - as well as longer imaging times to allow for the high mAs required for acceptable image noise [4].

In adult patients, dual energy CT utilizing a rapid switching technique has been shown to improve image quality at comparable radiation dose to mono-energetic CT. While image quality was improved, radiation doses remained high and the virtual monochromatic reconstructions required additional processing on a separate workstation [5].

There are several technical approaches to acquiring dual energy CTs available from different vendors, these include sequential acquisition of scans at different energies, rapid kV switching, multilayered detectors and dual source CT scanners [6]. Sequential scanning at two high and low potentials at different times has the limitation of degradation of image quality as the images are not acquired simultaneously. This limitation has been decreased by acquiring axial 180° data at each tube potential before moving the table. A second approach is to rapidly alternate the tube potential between alternate projection measurements. This requires a rapid transition time between high and low tube potentials to maximize energy separation. Dual energy CT scanners have been introduced that utilize multilayer detectors to acquire multi-energy data from a high tube current. The low energy data is acquired from the front detector layer and the high energy data from the back layer. Finally, there is dual energy dual source CT in which two X-ray tubes and detectors arrays are mounted on the same gantry approximately 90° to one another with one tube operated at the high potential and one at the low potential to acquire both energies nearly simultaneously.

In this study, we evaluated the use of dual energy CT scans of the head obtained on a dual source, dual energy CT scanner to reduce radiation while maintaining image quality in pediatric patients. Mixed energy reconstruction was used because it can be automatically generated by the scanner at time of CT acquisition without additional processing at a separate workstation.

## 2. Material and methods

### 2.1. Patients

In this institutional review board approved, retrospective study, the PACS at our institution was searched for CT scans of the head without contrast performed from two distinct, non-overlapping time periods (July–October 2014 and September–October 2015), on the Siemens Somatom Definition FLASH. Two time periods were utilized as a subset of the scans during the initial time period (> 6 year old dual energy) were reconstructed without iterative reconstruction (SAFIRE) utilized on all other helical and dual energy scans. Seventeen patients on whom SAFIRE iterative reconstruction was not performed were excluded from the analysis. During the initial time period, both scan protocols were used interchangeably and no set criteria was utilized to select patients for a particular technique. During the second time period, all scans were performed with the dual energy technique. The CT scans were divided into two different age groups, < 6 years of age and at/or > 6 years of age, as scanning parameters are different between these ages at our institution.

Of the 405 consecutive patients scanned during these two time periods, a random sampling of 150 patients was collected (random number between 0 and 1 assigned in Microsoft Excel to each scan and first 150 sequential random numbers selected).

As the study was performed to evaluate image quality, patients with significant abnormalities (e.g., postoperative patients, patients with severe hydrocephalus, and patients with large hemorrhages) were excluded. Seventeen patients on whom SAFIRE iterative reconstruction was not performed were also excluded from the analysis. A total of 75 out of these 133 CTs were evaluated. Of the total of 75 patients, 27 patients under 6 years of age and 17 patients over 6 years of age were scanned using the conventional protocol while 16 patients under

**Table 1**

CT technique.

	Helical 0–6	DE 0–6	Helical > 6	DE > 6
kVp	120	80/140Sn	120	80/140Sn
Quality reference mAs	290 (120 kV)	356 tube A 80 kV and 178 tube B Sn140 kV	320 (120 kV)	420 tube A 80 kV and 210 tube B Sn140 kV
CARE dose 4d	On	On	On	On
Collimation	0.6 mm	0.6 mm	0.6 mm	0.6 mm
Detectors	128	40	128	40
Pitch	1.0	0.7	1.0	0.7
Rotation	1.0 s	0.5 s	1.0 s	0.5 s
Scan time	4.7 s	8.4 s	4.7 s	8.4 s
SAFIRE	3	3	3	3
Anti-cupping	3	3	3	3

The chosen quality reference mAs is in regards to tube A with the quality reference mAs for tube B automatically selected by the scanner.

6 years old and 15 patients over 6 years old were scanned utilizing the dual energy protocol.

### 2.2. CT protocol

All scans were performed on a Dual Source Dual Energy CT scanner (Somatom Definition Flash, Siemens Healthcare, Forchheim, Germany). Helical head CTs were performed with 120 kVp, automatic tube current modulation (CARE Dose 4d), pitch of 1.0, rotation time of 1.0 s. Quality reference mAs (with reference kV of 120) of 290 was utilized in patients from 0 to 6 years of age and 320 in patient > 6 years of age (Table 1).

Dual energy CTs were performed at 80kVp and Sn140kVp where Sn indicates tin filtration of the high energy tube, automatic tube current modulation (CARE Dose 4d), pitch of 0.7, rotation time of 0.5 s. Quality reference mAs 356 tube A 80 kV and 178 tube B Sn140 kV for patients 0–6 years of age and 420 tube A 80 kV and 210 tube B Sn140 kV in patients > 6 years of age (Table 1).

### 2.3. Image processing

All reconstructions were performed using the Siemens iterative reconstruction technique (SAFIRE) at level 3 for both conventional and DE scans. Anti-cupping level 3 was enabled for all scans. Axial 3 mm soft tissue (J37s), axial 3 mm bone (J70h), sagittal soft tissue (J37s), coronal soft tissue (J37s) and axial 0.5 mm (J37s) reconstruction were generated on all conventional helical scans (Table 2).

Mixed DE reconstruction were utilized for 3 mm axial, sagittal and coronal reconstructions, these are generated automatically on the scanner as the scans were completed. Thin section 0.5 mm images at each energy (80 kV and Sn140kV) were also generated as this allows for additional reconstruction to be generated on an independent workstation. Mixed energy reconstruction were performed on all DE scans using the same ratio as described by the F number in the reconstructions below with the range being between –1 for 140 kV and 1 for 80 kV. Axial 3 mm soft tissue mixed with F.0.3 (J37f), axial 3 mm bone mixed with F.0.4 (J60h), sagittal soft tissue mixed with F.0.3 (J37f),

**Table 2**

CT reconstructions.

	Conventional	Dual energy
Axial brain	3 mm J37s	3 mm J37f F.0.3
Axial bone	3 mm J70h	3 mm H60f F.0.4
Sagittal brain	3 mm J37s	3 mm J37 F.0.3
Coronal brain	3 mm J37s	3 mm J37 F.0.3
Axial thin	0.5 mm J37s	0.5 mm 80kVp J37s 0.5 mm Sn140kVp J37s

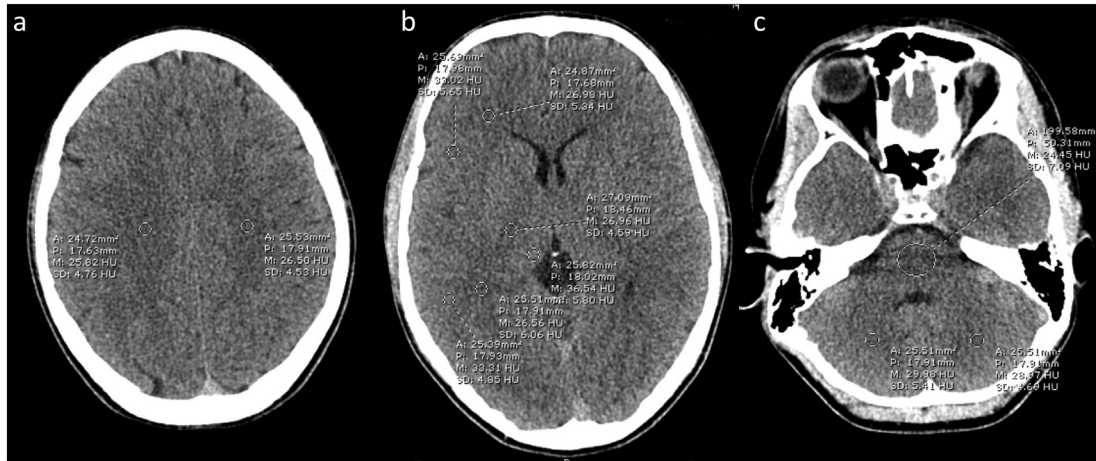


**Fig. 1.** ROI placement for quantitative analysis. All ROIs were 25 mm<sup>2</sup> except for interpetrous posterior fossa 200 mm<sup>2</sup> a Supratentorial brain ROIs were placed in posterior limb of the internal capsule, thalamus, posterior juxtacortical white matter, posterior cortex, anterior juxtacortical white matter, anterior cortex. b Centrum semiovale ROIs were placed in the bilateral centrum semiovale. c Posterior fossa ROIs were placed in bilateral cerebellar hemispheres and interpetrous region.

coronal soft tissue mixed with F\_0.3 (J37f), axial 0.5 mm 80 kV (J37s) and axial Sn140 kV (J37f) reconstruction were generated on all DE scans (Table 2). On patients with trauma indications, additional volume rendered reconstruction of the skull was generated for both conventional helical and DE scans.

2.4. Quantitative image quality

Quantitative analysis was performed using methodology similar to Pomerantz [5] and McKnight [7]. On the institution's PACS (Fuji Synapse PACS system 11), ROIs were drawn to measure mean and standard deviation (SD) of CT attenuation in Hounsfield units in the following anatomic locations: bilateral centrum semiovale, bilateral cerebellar hemispheres, bilateral posterior limbs of the internal capsules, bilateral thalami, bilateral anterior juxtacortical white matter, bilateral anterior cortex, and bilateral interpetrous regions of posterior fossa in area of highest beam hardening artifact (Fig. 1a, b, and c). ROI size was 25mm<sup>2</sup> +/1 mm in all regions and 200 mm<sup>2</sup> ± 5 mm in the interpetrous region of the posterior fossa as previously described (Fig. 1).

Attenuation values (HU) and noise (SD) for gray (anterior cortex, posterior cortex and thalamus) and white matter (centrum semiovale, posterior limb of the internal capsule, anterior juxtacortical white matter and posterior juxtacortical white matter) were averaged for comparison between conventional helical and DE scans.

Signal-to-noise ratios (SNRs) were calculated by dividing the mean CT number by its respective standard deviation (SD) for each of the ROIs detailed as well as for averaged gray and white matter.

Contrast-to-noise (CNR) was calculated using the formula: CNR = (mean attenuation of gray matter – mean attenuation of white matter)/[(SD<sub>GM</sub>)<sup>2</sup> + (SD<sub>WM</sub>)<sup>2</sup>]<sup>1/2</sup> [8].

2.5. Qualitative image quality

Three radiologists, blinded to the type of scan, qualitatively graded each CT scan in terms of noise, sharpness, and diagnostic acceptability within the infratentorial and supratentorial regions of the brain on predetermined, three- and four-point Likert scales. The Likert scale for noise was: 1 optimum; 2 little noise; 3 noisy but acceptable; 4 too much noise-uninterpretable. The scale for sharpness was: 1 well defined with sharp contours; 2 can be seen, contours sharp enough for diagnostic information; 3 structures visualized but non-diagnostic and contours blurred; 4 structures cannot be defined. The scale for diagnostic acceptability was: 1 fully acceptable; 2 acceptable but limited; 3

unacceptable.

2.6. Statistical analysis

To determine if the SD and SNR values within each ROI were significantly different between conventional and dual energy CTs, multivariable regression analysis with a gamma link function (to account for the fact that SD and SNR values never fall below zero) was utilized, with age of the child (in months) included as a potential confounding variable. For ROIs in which measurements were taken on both the left and right hemispheres (or in the anterior and posterior parts of the brain), a mixed model was utilized instead to account for correlation. All regression analyses were stratified by age-based protocols. To account for multiple comparisons, a Bonferroni correction was implemented.

Kendall's coefficient of concordance was calculated to assess the overall level of agreement between the three pediatric radiologists for the six Likert scales created. As agreement on an ordinal scale can be more difficult to obtain than on a categorical scale due to inherent biases within raters (e.g., a rater may be more likely to rate something at the extremes of the scale, etc.), the mode of the three ratings was taken; if no mode existed for a particular subject-scale combination, it was treated as missing. Using these modes, Fisher's exact tests were conducted to see if a significant association existed between the Likert scales and the conventional versus dual energy CTs. Again, these analyses were stratified by age-based protocols and a Bonferroni correction was implemented to account for multiple comparisons.

3. Results

3.1. Quantitative analysis

In patients < 6 years of age, the standard deviation, an un-normalized indicator of noise, was significantly less on dual energy scans in both the gray and white matter. However, there was no significant difference in the signal-to-noise ratios, contrast-to-noise ratio, or posterior fossa artifact index between standard and dual energy protocols (Table 3).

In patients at least 6 years of age, while signal-to-noise ratios were not significantly different between protocols, standard deviations were significantly smaller for the dual energy protocol, as well as the posterior fossa artifact index. The contrast-to-noise ratio was slightly, yet significantly, smaller in dual energy scans as compared to standard protocol, suggesting a mildly diminished contrast on the DE scans

**Table 3**  
Quantitative image quality comparison between conventional and dual energy CT in patients < 6 years.

Imaging quality index	Conventional CT	Dual energy CT	95% CI difference	P-value*
	Mean ± SD	Mean ± SD		
Gray matter HU	31.49 ± 0.50	29.70 ± 0.59	(0.85, 0.93)	< 0.0001
Gray matter HU noise	3.34 ± 0.07	3.09 ± 0.08	(0.81, 0.90)	< 0.0001
Gray matter HU SNR	9.49 ± 0.22	9.69 ± 0.28	(0.98, 1.11)	0.2042
White matter HU	23.62 ± 0.38	22.88 ± 0.46	(0.90, 0.98)	0.0051
White matter HU noise	3.09 ± 0.06	2.93 ± 0.07	(0.85, 0.95)	0.0002
White matter HU SNR	7.70 ± 0.15	7.86 ± 0.19	(0.99, 1.10)	0.1454
Gray-white matter contrast-to-noise ratio (CNR)	1.74 ± 0.09	1.63 ± 0.10	(0.76, 1.01)	0.0766
Posterior fossa artifact index	4.53 ± 0.15	4.41 ± 0.18	(0.86, 1.04)	0.2446

\* To account for multiple comparisons, a Bonferroni correction was implemented such that the significance level is now a P-value of ≤0.007.

**Table 4**  
Quantitative image quality comparison between conventional and dual energy CT in patients > 6 years.

Imaging quality index	Conventional CT	Dual energy CT	95% CI difference	P-value*
	Mean ± SD	Mean ± SD		
Gray matter HU	33.98 ± 0.94	32.06 ± 0.93	(0.86, 0.92)	< 0.0001
Gray matter HU noise	3.62 ± 0.22	3.41 ± 0.22	(0.82, 0.96)	0.0031
Gray matter HU SNR	9.63 ± 0.60	9.55 ± 0.62	(0.91, 1.07)	0.6819
White matter HU	26.62 ± 0.69	25.99 ± 0.70	(0.92, 0.98)	0.0042
White matter HU noise	3.21 ± 0.11	3.10 ± 0.11	(0.89, 0.98)	0.0028
White matter HU SNR	8.35 ± 0.30	8.42 ± 0.32	(0.97, 1.06)	0.4861
Gray-white matter contrast-to-noise ratio (CNR)	1.60 ± 0.15	1.43 ± 0.14	(0.71, 0.91)	0.0004
Posterior fossa artifact index	5.18 ± 0.53	4.57 ± 0.49	(0.68, 0.89)	0.0001

\* To account for multiple comparisons, a Bonferroni correction was implemented such that the significance level is now a P-value of ≤0.007.

relative to standard protocol scans (Table 4).

3.2. Qualitative analysis

Qualitatively, there was little difference in image quality in patients < 6 years old with the only significant difference in decreased/improved infratentorial noise on the DE scans (Fig. 2 and Table 5). In patients > 6 years of age, all infratentorial measures including noise, sharpness and diagnostic acceptability were significantly improved on the DE scans as was supratentorial sharpness and diagnostic acceptability (Fig. 3 and Table 5).

3.3. Radiation exposure

Radiation exposure as measured by CTDI and DLP was significantly lower on dual energy scans in both patient populations. In patients < 6 years old, CTDI was 19.6 mGy for the conventional scans and 18.4 mGy for the DE scans, a 6.1% reduction. DLP was reduced from 309.9 for conventional scans to 272.4 for DE scans, a 12.1% reduction. In patients over 6 years of age CTDI was 30.9 mGy for the conventional scans and 27.5 for the DE scans, a 11.0% reduction. DLP was reduced from 541.45 for conventional scans to 466.3 for DE scan, a 30.0% reduction (Table 6).

4. Discussion

Dual energy CT of the head is a robust technique that allows for optimization of image quality. This technique has been used in adults and shown to improve image quality with a similar to mildly increased radiation dose [5]. In this study, we describe a dual energy CT protocol in pediatric patients in which image quality is maintained or mildly improved while radiation dose is modestly reduced.

Obtaining a CT scan of the head at two different energies allows for the possibility of reconstructing the images at multiple different energies, thus optimizing different aspects of image quality. Data from a single dual energy acquisition could be reconstructed in different mixed

energy or monochromatic reconstructions to optimize different image quality metrics. For example, reconstructing the posterior fossa at a lower mixed energy ratio or higher kEv would decrease the streak artifacts related to the skull base that often limit evaluation of posterior fossa structures. Conversely, reconstructing at a higher mixed energy ratio or lower kEv could be used to maximize contrast in the supratentorial brain. Reconstructing DE CTs using advanced virtual monochromatic reconstructions has recently been described in children [9]. While the results are quite promising, at this time this requires reconstruction on dedicated independent workstation, often by a specially-trained technologist.

In our protocol, we focused on optimizing overall image quality with a set of reconstructions that were analogous to our conventional CT protocol. Scans were reconstructed using a mixed energy algorithm that is available on the CT scanner workstation. In order to generate mono energetic reconstructions, studies would need to be transferred to an independent workstation and the reconstruction performed manually. This is impractical for the typical busy practice, where a large number of head CTs are performed for the emergency department 24 h a day. Our protocol is reconstructed with little, if any, technologist intervention at the CT workstation and is utilized by all technologists at our institution.

Radiation exposure, as reported by decreased CTDI and DLP, was modestly decreased utilizing the DE protocol compared with the conventional CT protocol. This is not intrinsic to the DE technique, but rather is due to the protocol design by altering quality reference mAs and scan parameters. Also, the DE protocol only allows for 40 detectors to be utilized at each energy, as opposed to both banks of 64 detectors each (128 detectors total) being utilized in the conventional scan. This use of a narrower band of detectors for the DE protocol may account for some of the improvement in image quality. This also explains why there is a greater reduction in radiation exposure, as the difference is likely due to over ranging with the wider detector field in the conventional scan. A smaller block of detectors could be utilized in the conventional protocol to mitigate these effects, although this would partially eliminate the advantage in decreased scan time for the conventional

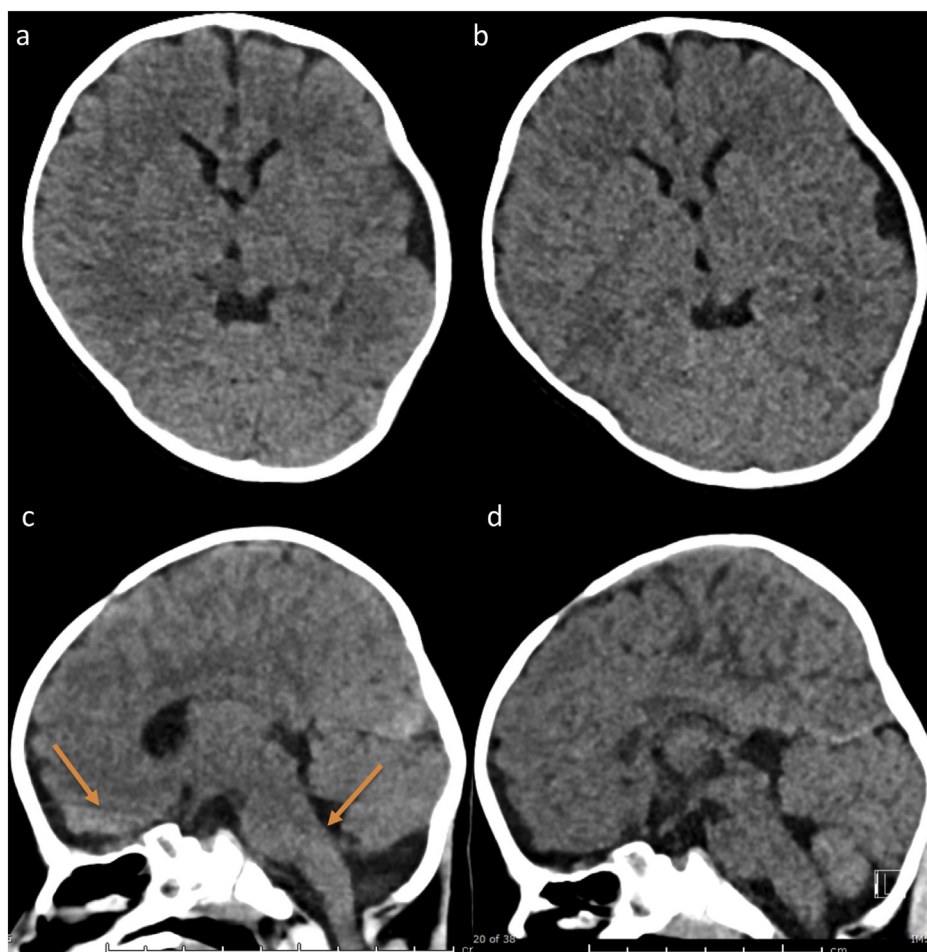


**Fig. 2.** Axial reconstructions from a Non contrast head CT obtained in a 5 month old patient with microcephaly and concern for congenital infection. b Non contrast dual energy CT in the same patient at 7 months of age performed for trauma with occipital swelling. Sagittal reconstructions demonstrate beam hardening artifact through the inferior frontal lobes and posterior fossa (arrows) on the conventional CT c that are not present on the dual energy CT d.

**Table 5**  
Qualitative image analysis using Kendall's coefficient of concordance and fisher's exact P-values testing associations between Likert scale and conventional versus dual energy CT.

Likert scale	Coefficient of concordance*	Fisher's exact P-value**	
		Under 6 years of age protocol	Over 6 years of age protocol
Infratentorial noise	0.576	0.003	0.001
Infratentorial sharpness	0.622	0.021	< 0.001
Infratentorial diagnostic acceptability	0.61	0.044	< 0.001
Supratentorial noise	0.495	0.128	0.068
Supratentorial sharpness	0.477	0.053	0.002
Supratentorial diagnostic acceptability	0.491	0.834	0.023

\* Correlates to moderate concordance for all tested measures except for infratentorial sharpness and diagnostic acceptability which have substantial concordance.

\*\* To account for multiple comparisons, a Bonferroni correction was implemented such that the significance level is now a P-value of  $\leq 0.007$ .

protocol.

An important disadvantage to the DE protocol is that the scans take longer to acquire, approximately 8.4 s versus 4.7 s for the conventional protocol. While this has the potential to lead to more failed or repeated exams, we have not experienced this subjectively. This data was not

directly collected or tested.

There are a few limitations to our study. No systematic randomization to dual energy or standard protocol was performed during the initial time period when both protocols were being utilized, so while we do not know of any selection bias, this cannot be entirely excluded. As our study was a retrospective comparison study using images obtained clinically at different times, we are unable to do a paired comparison of both types of CT obtained in the same patient. To try to minimize this limitation, all studies included in the analysis were performed on a single CT scanner to decrease any differences that may be due to the scanner system itself, such as differences in detectors, X-ray tube, data acquisition system, etc. Although identical reconstruction kernels are not available for DE and convention scans, closely analogous kernels were utilized and the remainder of the reconstruction parameter (slice thickness, SAFIRE, anti-cupping) were the same. To avoid confounding factors in evaluation of image quality, patients with obvious pathology were excluded and, hence, we cannot evaluate any effect change in image quality would have in evaluating different pathologic processes. A limitation of our study was the relatively small sample size utilized. Future studies would benefit from randomization to control or dual energy studies as well as a larger sample size.

Given the results of this study and radiologist preference, our department now utilizes dual energy scans on all head CTs performed on our dual energy scanner. We have added virtual non-contrast reconstructions to head CTs performed with contrast. Other reconstruction techniques including mono-energetic reconstructions and material decomposition have not yet been widely utilized.

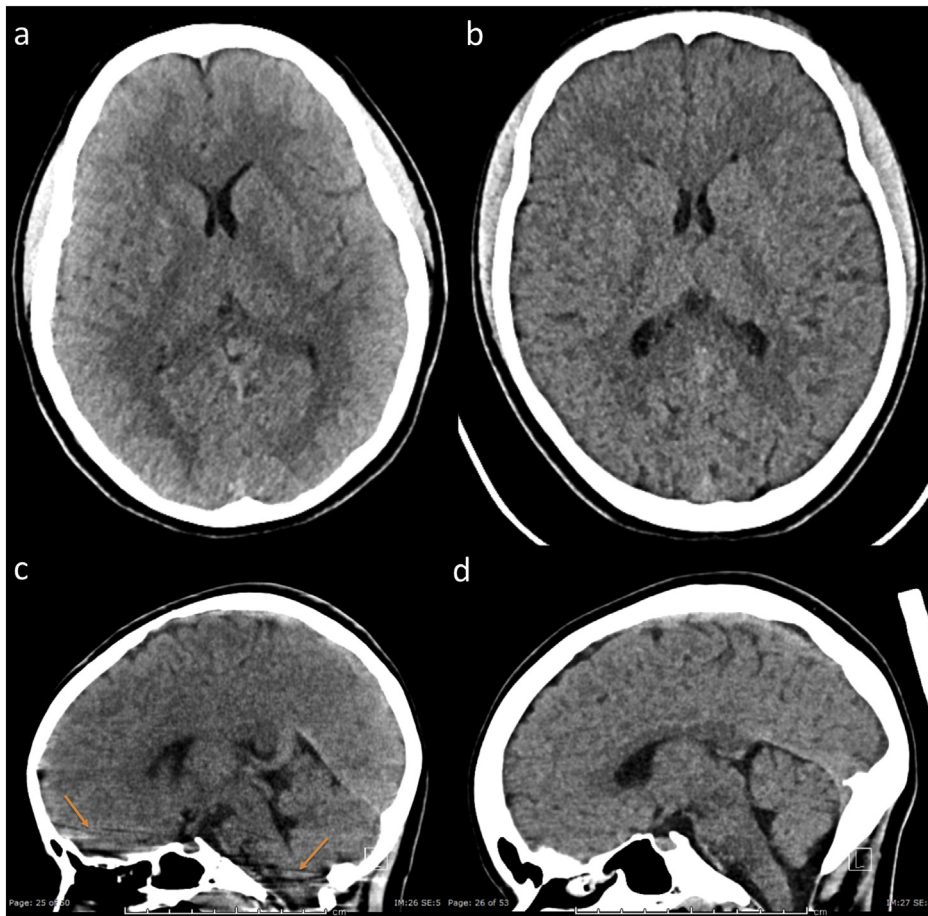


Fig. 3. Axial reconstructions from a Non contrast head CT obtained in a 17 year old patient with altered mental status. b Non contrast dual energy CT in a different 17 year old patient after minor trauma. Sagittal reconstructions demonstrate beam hardening artifact through the inferior frontal lobes and posterior fossa (arrows) on the conventional CT c that are significantly reduced on the dual energy CT d.

**Table 6**  
Radiation dose comparison between conventional and dual energy CT.

Image quality index	Age protocol	Conventional CT	Dual energy CT	P-value*
CTDI	Under 6 years of age	19.60 ± 0.42	18.43 ± 0.64	0.004
	Over 6 years of age	30.94 ± 0.85	27.53 ± 1.10	< 0.001
DLP	Under 6 years of age	309.91 ± 10.88	272.4 ± 15.51	< 0.001
	Over 6 years of age	541.45 ± 19.11	466.27 ± 23.98	< 0.001

\* To account for multiple comparisons, a Bonferroni correction was implemented such that the significance level is now a P-value of ≤0.007.

**5. Conclusion**

In this study, we demonstrate that dual energy head CT can be performed in clinical practice in pediatric populations with lower radiation exposure, mildly improved overall image noise and no significant decrease in signal-to-noise ratios. Further, subjective image quality is similar in patients under 6 years of age and improved in patients > 6 years. Dual energy scans also reduce artifacts at the skull base and posterior fossa compared to conventional CT. Given the results of our study, dual energy head CT is a viable alternative conventional CT in children.

**References**

[1] Curry T, Dowdey J, Murry R. Christensen's physics of diagnostic radiology. 4th ed. Philadelphia: Lea & Febiger; 1990.  
 [2] Huda Walter. Review of radiologic physics. Phys Med Biol 2010. <https://doi.org/10.1088/0031-9155/41/12/018>.  
 [3] Udayasankar UK, Braithwaite K, Arvaniti M, et al. Low-dose nonenhanced head CT protocol for follow-up evaluation of children with ventriculoperitoneal shunt:

reduction of radiation and effect on image quality. AJNR Am J Neuroradiol 2008;29:802–6. <https://doi.org/10.3174/ajnr.A0923>.  
 [4] Park JE, Choi YH, Cheon JE, et al. Image quality and radiation dose of brain computed tomography in children: effects of decreasing tube voltage from 120 kVp to 80 kVp. Pediatr Radiol 2017;47:710–7. <https://doi.org/10.1007/s00247-017-3799-8>.  
 [5] Pomerantz SR, Kamalian S, Zhang D, et al. Virtual monochromatic reconstruction of dual-energy unenhanced head CT at 65–75 keV maximizes image quality compared with conventional polychromatic CT. Radiology 2013;266:318–25. <https://doi.org/10.1148/radiol.12111604>.  
 [6] McCollough CH, Leng S, Yu L, Fletcher JG. Dual- and multi-energy CT: principles, technical approaches, and clinical applications. Radiology 2015;276:637–53. <https://doi.org/10.1148/radiol.2015142631>.  
 [7] McKnight CD, Watcharotone K, Ibrahim M, et al. Adaptive statistical iterative reconstruction: reducing dose while preserving image quality in the pediatric head CT examination. Pediatr Radiol 2014;997–1003. <https://doi.org/10.1007/s00247-014-2943-y>.  
 [8] Mullins ME, Lev MH, Bove P, et al. Comparison of image quality between conventional and low-dose nonenhanced head CT. Am J Neuroradiol 2004;25:533–8. [\[doi:15090337\]](https://doi.org/10.1007/s00247-017-3908-8).  
 [9] Park J, Choi YH, Cheon J-E, et al. Advanced virtual monochromatic reconstruction of dual-energy unenhanced brain computed tomography in children: comparison of image quality against standard mono-energetic images and conventional polychromatic computed tomography. 2017. p. 1648–58. <https://doi.org/10.1007/s00247-017-3908-8>.